Acta Geod Geophys (2016) 51:583–595
DOI 10.1007/s40328-015-0147-z

Radon emission evolution and rock failure

Qiang Sun[1] · Chunhu Zhao[2] · Hanjiang Lü[2]

Received: 2 June 2015 / Accepted: 17 October 2015 / Published online: 28 October 2015

Abstract Previous experimental studies showed that the variation of Radon (Rn) emission is closely related to the development of rock deformation: Rn emission has a rapid increase with the growth of cracks and their surface areas (i.e. onset of fracture coalescence point), and reaches the maximum at rock failure. In this study, the stress level at the onset of fracture coalescence λ_c is predicted with the renormalization group theory. It is assumed that rock is a strain-softening medium whose strength can be described by Weibull's distribution. Result shows that λ_c depends mainly on the homogeneity index or shape parameter m in the Weibull's distribution for the rock. Both experimental and analytical results show that this point of rapid increase in Rn emission on the Rn-strain curve corresponds to the critical point on the stress–strain curve; for rock compression, the stress at this point is approximately 70–80 % of the peak strength. Hence a generalized crack damage threshold is proposed in the present study based on the characteristics of Rn emission during the loading process, for recognizing the critical point of rock fracture.

Keywords Rock failure · Critical information · Rn emission · Identification

1 Introduction

Studying the mechanical behavior of rock failure based on its stress–strain curve and other physical parameters has important scientific and engineering values (Chen and Lin 2004). Variation of rock cracking or porosity under an external load can affect the rock's stress–

✉ Qiang Sun
sunqiang04@126.com

[1] School of Resources and Geosciences, China University of Mining and Technology, Xuzhou 221116, Jiangsu, People's Republic of China

[2] Xi'an Research Institute, China Coal Technology and Engineering Group, Xi'an 710054, Shanxi, People's Republic of China

strain state and other physical parameters (i.e. ElectroMagnetic emission energy (EME), Dou et al. 2007), velocity (Chen et al. 1990), and resistivity (Figs. 1, 2, 3), and variations in these parameters can reflect the development of rock failure. From Figs. 1, 2 and 3, it is easy to see that the EME, velocity, and resistivity have significantly changing at point C (roughly corresponding to the yield point).

The fracturing of stressed materials is analogous to the critical phenomenon at a second-order phase transition or the percolation phenomenon (Herrmann and Roux 1990; Sornette 2000). The moment of rupture can be regarded as a critical point, so the fracturing process can be described with a renormalisation-group scheme (Anifrani et al. 1995). In a region in the vicinity of the critical point of rupture (Sornette and Andersen 1998), the variations in free energy, which is reflected in the released energy, can be characterised by a power law decorated by log-periodic oscillations (Sornette 1998).

In this study, we select the Rn emanation of rock as the internal variable, and three parameters, "stress level (normalized relative to the compressive strength), strain level (normalized relative to the axial strain threshold at the uniaxial compressive strength) and Radon emanation density", are used in the measurement and the state equations of rock. Rn is the only radioactive gas in nature. Its radioactivity comes from the following reaction

$$\underset{3.8\text{ d}}{^{222}\mathrm{Rn}} \xrightarrow{\vec{\alpha}} \underset{3.1\text{ min}}{^{218}\mathrm{Po}} \xrightarrow{\vec{\alpha}} \underset{21.6\text{ min}}{^{214}\mathrm{Po}}$$

The radioactivity of Rn is related to its atomic mass, atomic number and ionization energy. Rn has the largest atomic mass and atomic number among the six rare gases (i.e. He, Ne, Ar, Kr, Xe, and Rn), but the lowest ionization energy, as shown in Fig. 4. It is widely distributed in nature, i.e. in all kinds of rock, gypsum, concrete, sand, and water. In rock, Rn exists in three forms, including freedom, adsorption and sequestration (Wang 1990, 2010).

In most geological hazards (e.g. earthquake, landslide, rock collapse and inrush of coalmine), the development of cracks in rock plays an important role. Variations in Rn emanation have been considered as a possible precursory phenomenon for evaluating the deformation and fracture feature of rocks (Zhou et al. 1981). Significant achievements have been made in systematic studies on the variation of Rn emission with rock cracking (Luo

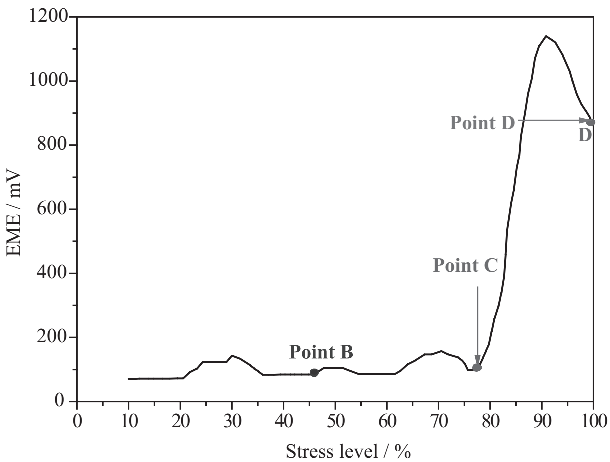

Fig. 1 Variation of electroMagnetic emission energy (EME) during pre-peaking phase of raw coal in Dongtan Mine (Dou et al. 2007)

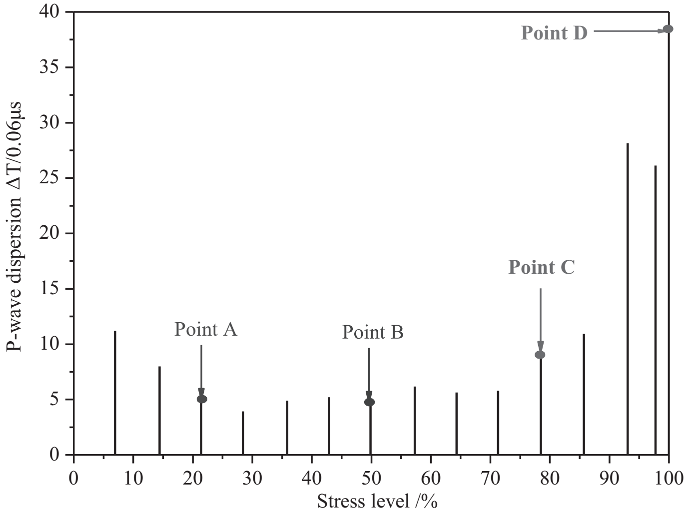

Fig. 2 Relationship between travel times of P-wave versus stress level in marble sample (Chen et al. 1990)

and Shi 1980; Holub and Brady 1981; Luo et al. 1981, 1984; Kies et al. 2005). Holub and Brady (1981) pointed that a generating mechanism of the Rn concentration anomalies in the co-seismic rupture was possibly enlargements of effective area of grain surface, porosity and radon emanation rates, which resulted from co-seismic cracking of rocks. Increase of Rn emission was found to generally start when the applied stress reaches 20–90 % of the corresponding failure stress, probably caused by the occurrence and growth of dilatant microcracks in rock (Zhou et al. 1981), which leads to increased emanation (King and Luo 1990). Kies et al. (2005) also proposed that variable volumetric strain and stress had important influence on the radon concentrations. Detecting the variation of Rn emission has been used in disaster geology (Wang 2010) and predicting earthquakes (Luo et al. 1984; Li et al. 1984; Crockett et al. 2006; Zhou et al. 2010).

This paper is a generalization and extension of previous studies. In this study, based on fracture mechanics, we introduce a few key concepts for understanding the evolution of Radon emission at a critical point on the stress–strain curve, and develop a renormalisation-group method to indirectly predict the occurrence of rock fracture.

2 Rn emission evolution and stress–strain of intact rock under compression

Rocks inevitably contain pores, flaws or microcracks. For example, weak grain boundaries may serve as sources of cracking. Microcracks will grow when the rock is loaded beyond a certain threshold, which is also reflected in the evolution of Rn emission.

Several characteristic stress levels identified in laboratory tests are important to understanding the failure of rock. They are shown as the stress–strain relation in Fig. 5: σ_a is the crack closure stress level; σ_b is the crack initiation stress level; σ_c is the crack damage stress level corresponding to long-term rock strength (Martin 1993, 1997) (i.e., the critical stress level), and σ_d is the peak stress. Rn emission events start to increase at σ_b and

Fig. 3 Relationship between resistivity and stress level. **a** Sandstone 2# (Lu et al. 1992); **b** No. 8 coal petrography (Li et al. 1999)

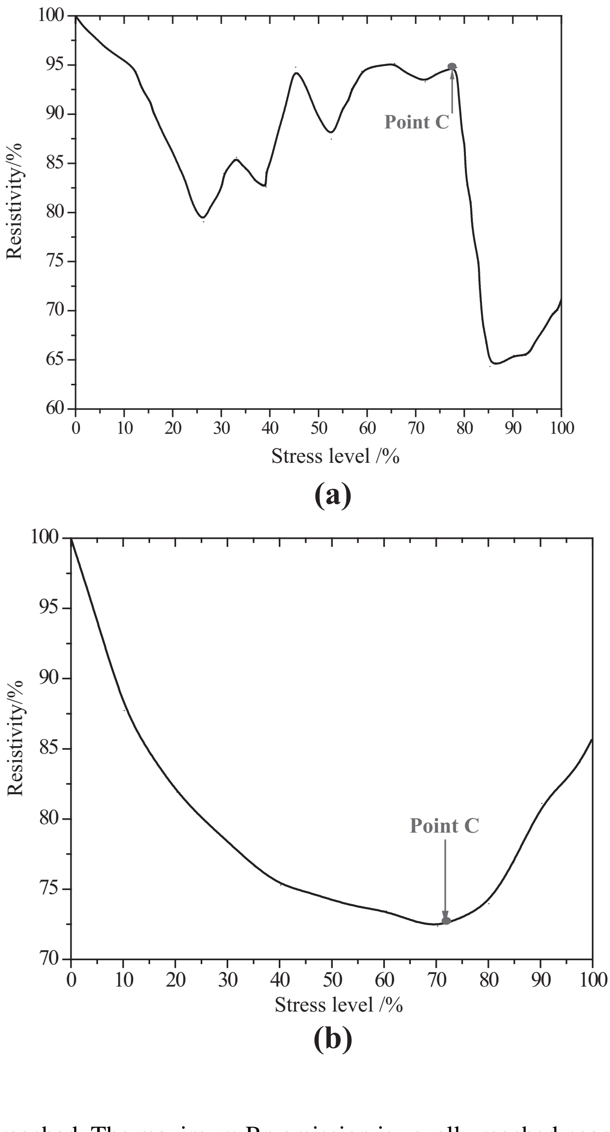

increase drastically when σ_c is reached. The maximum Rn emission is usually reached near σ_e, which is at the turning point of the constitutive curve. Three stress levels σ_b, σ_c, and σ_d, represent important stages in the development of macroscopic failure of intact rock (Martin 1997; Cai et al. 2004; Xue 2011).

The following characteristics of microcracking, Rn emission and rock failure have been found in previous studies:

(1) Rn emission increases at stress levels approximately 0.3–0.5 times the peak uniaxial load (Figs. 5, 6, 7).

(2) Microcracks form or propagate mainly in the direction parallel to the maximum compressive stress. This is evident from the measured volumetric strain dilatation (Martin 1997) and direct microscopic observation of test samples.

Fig. 4 Atomic weight and atomic number versus ionization energy of rare gases

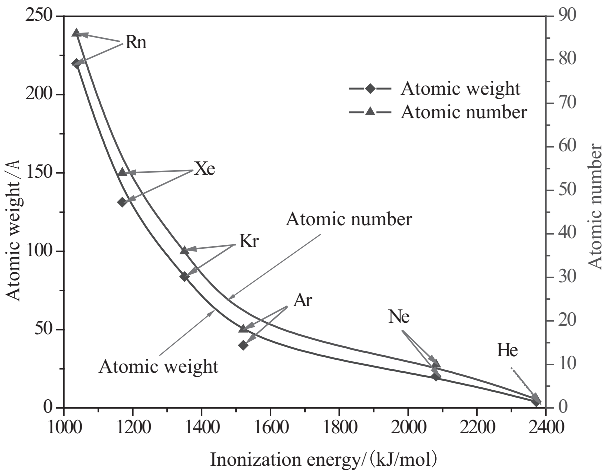

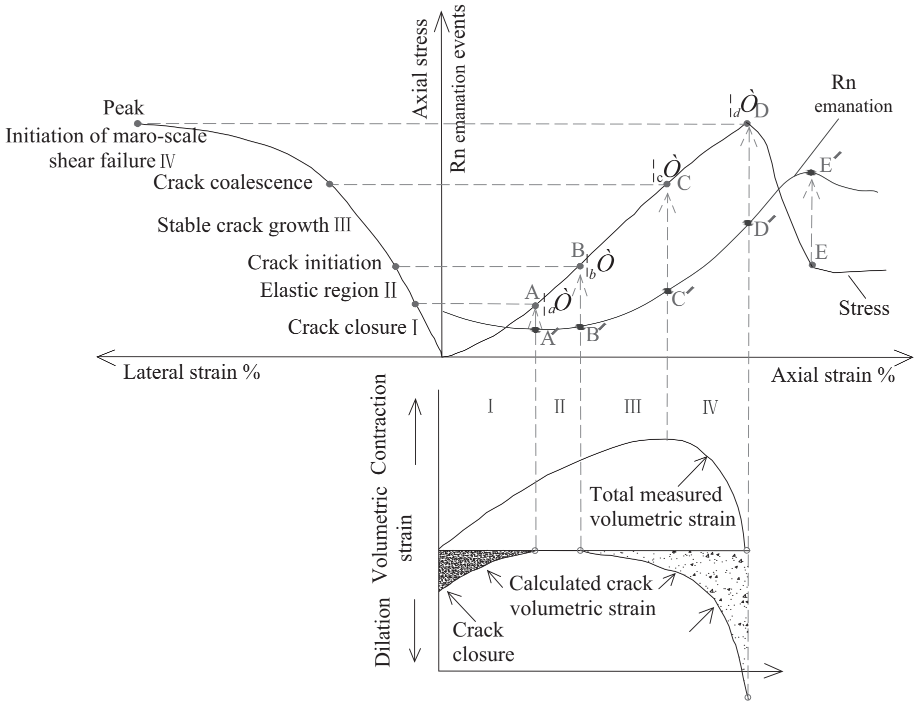

Fig. 5 Stress–strain diagram showing the stages of crack development by Rn emission [after Martin et al. (2001) and Cai et al. (2004)]

(3) Onset of fracture coalescence starts at stress levels approximately 0.7–0.8 times the peak strength (Lockner et al. 1992).

(4) Macrocracks or shear bands normally form after the peak strength is reached.

Fig. 6 Relationships between Rn emanation versus time in the loading process of rock materials. **a** The impact of loading to Rn emission (Luo et al. 1981). **b** Results of pressure related Rn experiment with no water (Li et al. 1984)

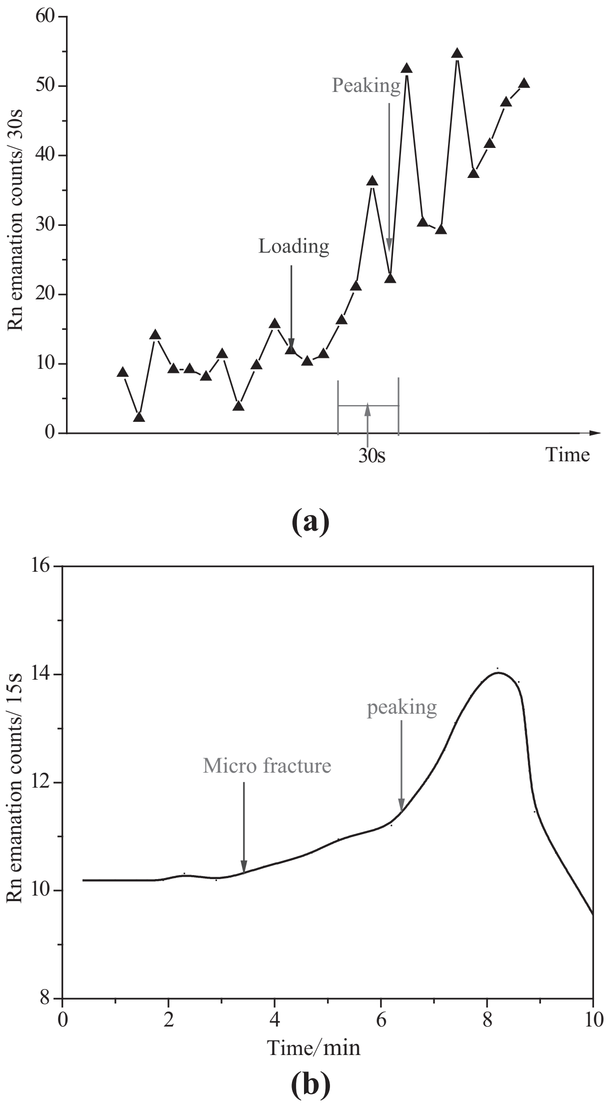

Based the Rn emission change versus stress level (Figs. 6, 7) obtained from experiments on rock samples, the variation of Rn emission with stress level can be separated into 3 phases. (1) In the compaction and elastic phases, there is a mixed trend in Rn emission with the increasing of stress. The Rn emission starts increasing at Point B, when stress level reaches 30–60 % of the peaking stress. (2) After the point B, with the increase of loading, micro cracks appear and gradually expand. In this process, the Rn emission increases. (3) Nearly to the Point C, plenty of micro cracks initiate and grow rapidly, and micro breaking is developed spatially in rows along the potential breaking planes until the microcracks eventually become connected with each other (Figs. 6, 7, 8), as indicated by the

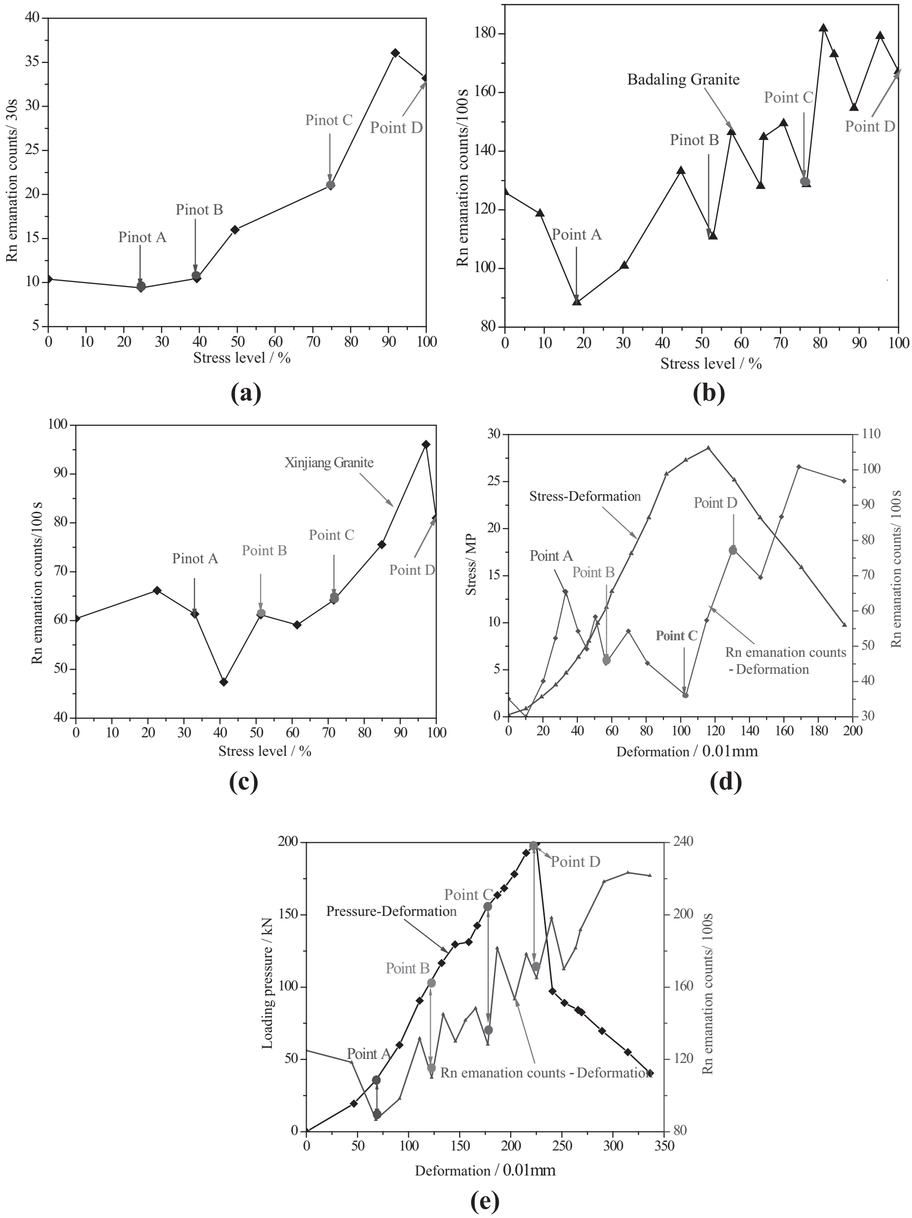

Fig. 7 Relationships between Rn emanation versus stress level during loading process. **a** Concrete (Luo et al. 1981); **b** badaling granite (Luo et al. 1981); **c** granite (Luo et al. 1981); **d** concrete (Luo et al. 1981); **e** badaling granite (Luo and Shi 1980)

localization of strain, and accelerated increase of volumetric strain at the cracks. In this phase, the Rn emission is increasing steeply.

Rn emission generally increases with the growth of cracks. In laboratory tests, σ_b (the crack initiation stress or threshold) is defined as the onset of stable growth of cracks, or the

Fig. 8 Relationships between Rn emanation versus stress and average volumetric strain versus stress level in loading process of concrete (Zhou et al. 1981). **a** No. 4, **b** No. 5

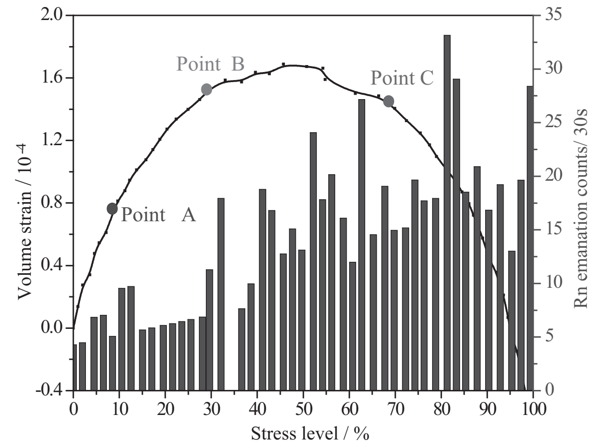

(a) No.4

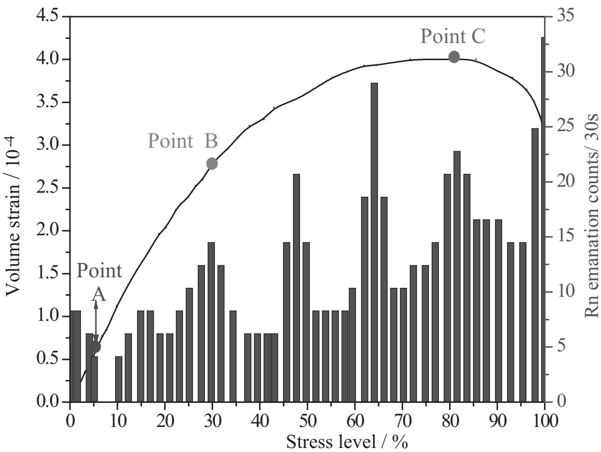

(b) No.5

stress level when crack volumetric strain deviates from zero. In some cases, testing samples may have been damaged in the course of preparation, so Rn emission can be detected at the crack closure stage. For this reason, Rn emission events recorded during the crack closure must be subtracted from the total cumulative count to avoid confusion in data analysis, when accumulated Rn emission counts are used to study the crack initiation and crack damage stress levels (Fig. 8).

The crack damage stress is generally defined as the stress level when volumetric strain reversal occurs and unstable growth of crack begins. Rn emission increases with the growth of pore surface during rock failure (Wang 2010). Under the vibration condition, Rn emission increases drastically, as shown in Fig. 9 (Luo et al. 1984). Existing cracks start to propagate and new cracks initiate in a stable fashion when the damage initiation limit is exceeded, but critical rock mass damage is only encountered when crack density is sufficient for cracks to coalesce and form shear band or tensile spalls. This state is defined as

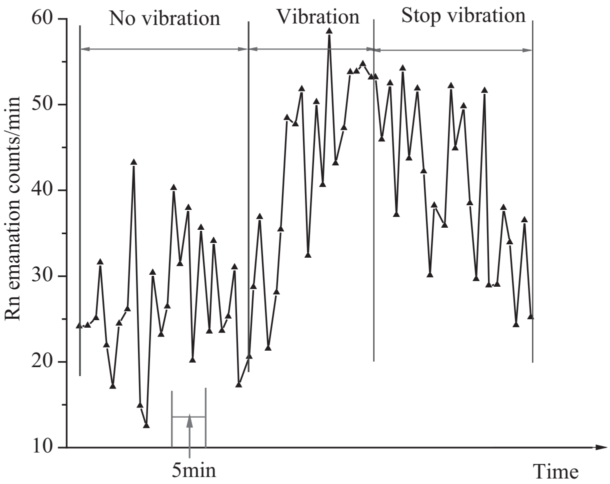

Fig. 9 Relationships between Rn emanation versus time in the vibration process of Liaoxi granite (Luo et al. 1984)

the "crack damage stress" (Martin 1997) or "Rn emission damage threshold" because in general, a single Rn emission can be viewed as a cracking event. Therefore, the crack damage stress also corresponds to the stress when drastic increase of Rn emission activity (the slope of the accumulated Rn emission events increases sharply) is observed.

In laboratory tests (Xue et al. 2014a, b), the crack damage stress level σ_c increases with the level of confinement. Hence, the unconfined σ_c determines the onset of failure propagation process in the field. In other words, σ_c can be considered as the "wall rock strength" in massive rocks. Table 1 summarizes some of the crack initiation and crack damage stress levels obtained from uniaxial and triaxial compression tests. In triaxial tests, the stress levels are defined by the deviatoric stress ($\sigma_1 - \sigma_3$). It can be found that the σ_b/σ_d ratio varies between 32 and 54 % and the σ_c/σ_d ratio varies between 70 and 81 %.

3 Prediction of the probability of critical rock failure

Table 1 shows that the measured stress level at the threshold point of destruction C ranges from about 70 to 80 % for most samples. In this section, we develop a theoretical method to indirectly predict the probability of critical rock failure.

Table 1 Summary of crack initiation and crack damage stress levels from laboratory test by Rn emission

Rock type	σ_b/σ_d (%)	σ_c/σ_d (%)	References
Concrete	32.1	81.0	Zhou et al. (1981)
Concrete	30.9	70.1	Zhou et al. (1981)
Concrete	39.3	74.5	Luo et al. (1981)
Badaling granite	44.7	76.7	Luo et al. (1981)
Xinjiang granite	41.1	71.6	Luo et al. (1981)
Badaling granite	54.1	78.7	Luo and Shi. (1980)

Based on the Weibull distribution, Qin et al. (2008, 2010a, b) used the classical Weibull's distribution to represent the probability p_α that the failure strength σ_f of a block is less than the stress $\alpha\sigma$

$$p_\alpha = p(\sigma_f < \alpha\sigma) = 1 - \exp\left[-\left(\frac{\alpha\sigma}{\sigma_0}\right)^m\right], \tag{1}$$

where σ is stress; α is the scale parameter; σ_0 is a measurement of average strength; and m is the shape parameter, a measurement of the variability of rock strength.

The failure probability of elementary blocks corresponding to $\alpha = 1$ can be expressed as

$$p_1 = p(\sigma_f < \sigma) = 1 - \exp\left[-\left(\frac{\sigma}{\sigma_0}\right)^m\right] \tag{2}$$

Combining Eq. (1) with Eq. (2), one has

$$p_\alpha = 1 - (1 - p_1)^{\alpha^m} \tag{3}$$

The conditional probability $p_{a,b}$ that failure will occur (Allegre et al. 1982) when the stress $(a - b)\sigma$ is transferred to an unbroken block supporting a stress $b\sigma$, can be written as

$$p_{a,b} = \frac{p(b\sigma < \sigma_f < a\sigma)}{p(\sigma_f > b\sigma)} = \frac{P_a - P_b}{1 - P_b} \tag{4}$$

If critical damage phenomenon exists in the loading process of rock, then the failure probability $P^* = f(m)$ can be expressed as

$$f(m) = p^* = 1 - 0.5^{\frac{1}{2^m - 1}} \tag{5}$$

Equation (2) could be expressed as a probability function of strain, that is,

$$P = 1 - \exp\left[-\left(\frac{\varepsilon}{\varepsilon_0}\right)^m\right], \tag{6}$$

where, ε is the axial strain of the rock and ε_0 is the average strain.

Here, the stress–strain constitutive model of the rock can be expressed as:

$$\sigma = E_0\varepsilon \exp\left[-\left(\frac{\varepsilon}{\varepsilon_0}\right)^m\right], \tag{7}$$

where E_0 is the initial elastic modulus. By solving the first derivative for Eq. (7) with respect to the stress ε, the strain value corresponding to the peak strength is

$$\varepsilon_d = \left(\frac{1}{m}\right)^{1/m} \varepsilon_0 \tag{8}$$

Substitute (2) into Eq. (8), then the strain at the critical failure point C can be written as

$$\varepsilon_c = \left(\frac{\ln 2}{2^m - 1}\right)^{1/m} \varepsilon_0 \tag{9}$$

Divide Eq. (9) by Eq. (8), then we have

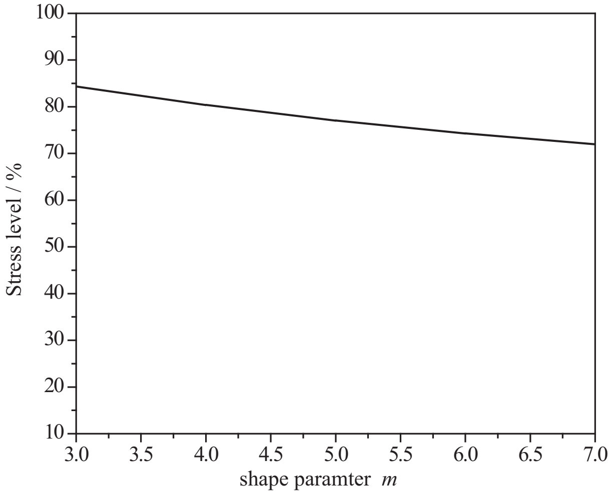

Fig. 10 The variation of the critical stress level with the shape parameter

$$\lambda_c = \frac{\sigma_c}{\sigma_d} \times 100\ \% = \left(\frac{m \ln 2}{2^m - 1}\right)^{1/m} \exp\left[\frac{1}{m} - \frac{\ln 2}{2^m - 1}\right] \times 100\ \% \quad (9)$$

The relationship between stress ratio of σ_c/σ_d and shape parameter m is shown in Fig. 10.

This renormalization group probability of destruction is then employed to calculate the stress at the threshold point and the stress corresponding to the peak strength, which are shown and compared with the experimental results in Table 1. The predicted onset of fracture coalescence occurs at stress of approximately 70–80 % times the peak strength, agreeing with the statistical mean of the range of stress level for sharp increase of Rn emission collected from laboratory samples. Hence, Rn emission could be used to indentify the range of critical point C in the stress–strain curve.

4 Conclusions

Investigating the crack damage in rocks by fracture mechanics and statistical physics, we found that the stress at critical point on the stress–strain curve is closely related to the point of rapid increasing on the Rn emission. We can use the variation of Rn emission to obtain the end stress of rock elastic stage (corresponds to point B), threshold point (corresponds to point C) and poisson's ratio.

We define σ_c and σ_d as the critical stress and peaking stress, and λ_c as the critical stress level of σ_c/σ_d. The predicted critical stress is approximately 70–80 % times the peak strength, agreeing with the statistical mean of the range of stress level for sharp increase of Rn emission collected from laboratory samples.

Hence a generalized crack damage threshold is proposed in the present study based on the characteristics of Rn emission during the loading process, which can be used as an internal variable characterizing the information on porosity change and information source to recognize the critical point of rock failure.

Acknowledgments This research was supported by the State Basic Research and Development Program of China (No. 2013CB036003), the Priority Academic Program Development of Jiangsu Higher Education Institutions, Transport project of China (2013318J12330) and the National Science Youth Foundation of China (41102201).

References

Allegre CJ, Le Mouel J L, Provost A (1982) Scaling rules in rock fracture and possible implications for earthquake prediction. Nature 297:47–49

Anifrani JC, Lefloch C, Sornette D, Souillard B (1995) Universal log-periodic correction group scaling for rupture stress prediction from acoustic emission. J Phys I (France) 5:631–638

Cai M, Kaisera PK, Tasaka Y, Maejima T (2004) Generalized crack initiation and crack damage stress thresholds of brittle rock masses near underground excavations. Int J Rock Mech Min Sci 41:833–847

Chen GY, Lin YM (2004) Stress-strain-electrical resistance effects and associated state equations for uniaxial rock compression. Int J Rock Mech Min Sci 41:223–236

Chen Y, Yang XW, Han B (1990) Spatial velocity variations of P waves during rock deformations. Acta Seismol Sin 12(1):54–59 **(in Chinese)**

Crockett RGM, Gillmore GK, Phillips PS, Denman AR, Groves-Kirkby CJ (2006) Radon anomalies preceding earthquakes which occurred in the UK, in summer and autumn 2002. Sci Total Environ 364:138–148

Dou LM, Wang YH, He XQ (2007) Study on electromagnetic emission characteristic for coal sample deformation and failure during pre-and post-peaking phases. Chin J Rock Mech Eng 26(5):908–914 **(in Chinese)**

Herrmann HJ, Roux S (1990) Statistical models for the fracture of disordered media. North-Holland, Amsterdam

Holub RF, Brady BT (1981) The effect of stress on Radon emanation from rock. J Geophys Res 86(B3):1776–1784

Kies A, Massen F, Tosheva Z (2005) Influence of variable stress on underground radon concentrations. Radioact Environ 7:334–334

King CY, Luo GW (1990) Variations of electric resistance and H_2 and Rn emissions of concrete blocks under increasing uniaxial compression. Pure Appl Geophys 134:45–56

Li GR, Jiang FL, Melvin J (1984) Experimental studies on responsible mechanisms for radon and some geochemical precursors. Seismol Geol 6(1):41–46 **(in Chinese)**

Li DC, Ge BT, Shu JS (1999) Experiment of resistivity variation of rocks in failure process. J China Univ Min Technol 28(5):491–493 (**in Chinese**)

Lockner DA, Byerlee JD, Kuksenko V et al (1992) Observation of quasi-static fault growth from acoustic emissions. In: Evans B, Wong TF (eds) Fault mechanics and transport properties of rocks. Academic Press, New York, pp 3–31

Lu YQ, Qian JD, Zhao JL et al (1992) Preliminary research on induced polarization effect before rupture of instable rocks. Earthquake 12(4):28–36

Luo GW, Shi XZ (1980) Experimental results of radon and thorium emanations from rock specimen under pressure. Acta Seismol Sin 2(2):198–204 (**in Chinese**)

Luo GW, Shi XZ, Wang JH (1981) Experimental results of the variations of several kinds of chemical parameters in process of specimen rupture under uniaxial compression. Acta Geophys Sin 24(1):117–122

Luo GW, Mu SL, Dong FC (1984) Observations of the radon and thorium emanation from Granite at audiofrequency vibration. Earthquake 13(5):21–22 **(in Chinese)**

Martin CD (1993) The strength of massive Lac du Bonnet granite around underground opening. PhD thesis, University of Manitoba

Martin CD (1997) Seventeenth canadian geotechnical colloquium: the effect of cohesion loss and stress path on brittle rock strength. Can Geotech J 34(5):698–725

Martin CD, Christiansson R, Söderhäll J (2001) Rock stability considerations for siting and constructing a KBS-3 repository. Based on Experiences from Äspö HRL, AECL's URL, tunneling and mining. SKB TR0138, Svensk Kärnbränslehantering AB

Qin SQ, Wang SJ, Sun Q, Xu GC, Ma P, Wang YY (2008) Foundation of nonlinear theory to rock and soil mechanics. Geologic Publishing House Press, Beijing **(in Chinese)**

Qin SQ, Wang YY, Ma P (2010a) Universal laws of critical displacement evolution for landslides and avalanches. Chin J Rock Mech Eng 29(15):873–880 **(in Chinese)**

Qin SQ, Xu XW, Hu P (2010b) Brittle failure mechanism of multiple locked patches in a seismogenic fault system and exploration on a new way for earthquake prediction. Chin J Geophys 53(4):1001–1014 **(in Chinese)**

Sornette D (1998) Discrete scale invariance and complex dimensions. Phys Rep 29(7):239–270

Sornette D (2000) Critical phenomena in natural sciences: chaos, fractals, selforganization and disorder: concepts and tools. Springer Series in Synergetics, Berlin, pp 257–284

Sornette D, Andersen JV (1998) Scaling with respect to disorder. Eur Phys J B 1:353–357

Wang YC (1990) Decay mechanism of groundwater (Gas) as carrier of the change in radon concentritions. N Chin Earthquake Sci. 8(1):69–75 **(in Chinese)**

Wang JF (2010) Radon migration in overlying strata during spontaneous combustion of coal underground and its application. Ph.D. Thesis, Taiyuan University of Technology, Taiyuan (**in Chinese**)

Xue L (2011) Renormalization study on rock failure and its application to strong earthquake prediction. Ph.D. Thesis, Institute of Geology and Geophysics Chinese Academy of Sciences, Beijing (**in Chinese**)

Xue L, Qin SQ, Sun Q, Wang YY, Qian HT (2014a) A quantitative criterion to describe the deformation process of rock sample subjected to uniaxial compression: from criticality to final failure. Phys A 410:470–482

Xue L, Qi M, Qin SQ, Li GL, Li P, Wang MM (2014b) A potential strain indicator for brittle failure prediction of low-porosity rock: Part I—experimental studies based on the uniaxial compression test. Rock Mech Rock Eng. doi:10.1007/s00603-014-0675-9

Zhou RG, Luo GW, Shi XZ (1981) The effect of loading rate on strength and failure mechanism of rocks. Chin J Geol 2(4):198–204

Zhou XC, Du JG, Chen Z, Cheng JW, Tang Y, Yang LM, Xie C, Cui YJ, Liu L, Yi L, Yang PX, Li Y (2010) Geochemistry of soil gas in the seismic fault zone produced by the Wenchuan Ms 8.0 earthquake, southwestern China. Geochem Trans 11(1):1–10